Photochemical & Photobiological Sciences

Accepted Manuscript

This is an *Accepted Manuscript*, which has been through the Royal Society of Chemistry peer review process and has been accepted for publication.

Accepted Manuscripts are published online shortly after acceptance, before technical editing, formatting and proof reading. Using this free service, authors can make their results available to the community, in citable form, before we publish the edited article. We will replace this *Accepted Manuscript* with the edited and formatted *Advance Article* as soon as it is available.

You can find more information about *Accepted Manuscripts* in the Information for Authors.

Please note that technical editing may introduce minor changes to the text and/or graphics, which may alter content. The journal's standard Terms & Conditions and the Ethical guidelines still apply. In no event shall the Royal Society of Chemistry be held responsible for any errors or omissions in this *Accepted Manuscript* or any consequences arising from the use of any information it contains.

ROYAL SOCIETY OF CHEMISTRY

www.rsc.org/pps

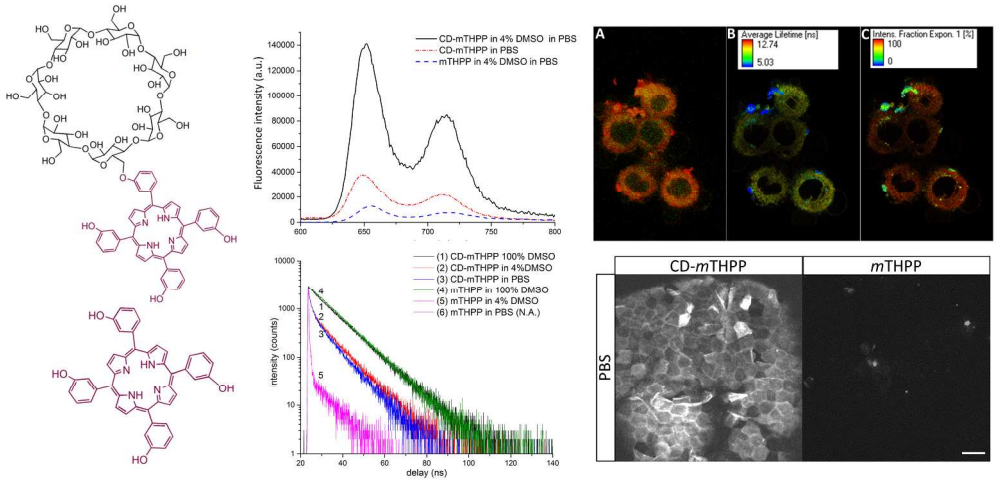

241x117mm (300 x 300 DPI)

Photochemical & Photobiological Sciences

ARTICLE

Cite this: DOI: 10.1039/x0xx00000x

Received 00th March 2014
Accepted 00th May 2014

DOI: 10.1039/x0xx00000x

www.rsc.org/

Photophysics and *ex vivo* biodistribution of β-cyclodextrin–*meso*-tetra(*m*-hydroxyphenyl)-porphyrin conjugate for biomedical applications

V. Kirejev,[a*] AR. Gonçalves,[b] C. Aggelidou,[b] I. Manet,[c] J. Mårtensson,[d] K. Yannakopoulou[b] and MB. Ericson[a*],

Low aqueous solubility of porphyrin-based photosensitizers hampers their clinical use in photodynamic therapy because of complex delivery. In this study, we explore *meso*-tetra(*m*-hydroxyphenyl)-21,23H-porphyrin (*m*THPP), a potent photosensitizer, covalently attached to β-cyclodextrin (CD-*m*THPP) with a focus on topical delivery and cellular uptake. The photophysical properties of CD-*m*THPP were examined using steady-state fluorescence and lifetime measurements verifying increased aqueous solubility. Confocal and fluorescence lifetime imaging microscopy on human squamous carcinoma cells (A431) evidenced a cytoplasmic uptake of CD-*m*THPP in predominantly monomeric form. CD-*m*THPP was also delivered to human skin *ex vivo* and the skin penetration was assessed using two-photon fluorescence microscopy. The results indicated that CD-*m*THPP exhibits improved skin distribution compared to *m*THPP alone using aqueous vehicles. Thus the CD-*m*THPP conjugate demonstrates improved biodistribution *ex vivo* compared to *m*THPP and is a promising multimodal system for photodynamic therapy.

Introduction

Porphyrins are photoactive compounds of broad scientific interest and have applications in several fields, among which photomedicine stands out. Specifically, porphyrins are extensively explored as photosensitizers in photodynamic therapy (PDT). The lipophilic character of many porphyrins represents a challenge for their application in clinical PDT as aqueous drug delivery systems are preferred [1-3]. Indicative of this limitation is that few porphyrin-based photosensitizing agents are currently approved for clinical use [4]. PDT constitutes an important therapy in dermatology [5, 6]; however, the challenging delivery of photosensitizers hampers the translation of PDT for additional oncological applications. Meso-tetra(m-hydroxyphenyl)porphyrin (*m*THPP) is the porphyrin analogue of the clinically approved photosensitizer meso-tetra(m-hydroxyphenyl)chlorin (*m*THPC, a.k.a. temoporfin commercialized, under the name Foscan®), and its photosensitizing properties have been confirmed [7-9]. Both *m*THPP and *m*THPC have proven to be 25 to 30 times more potent than photosensitizers compared to the hematoporphyrin derivatives; e.g., Photofrin, *in vivo* [10]; however, like other porphyrin compounds, they suffer from poor aqueous solubility, forming non-fluorescent aggregates in water solution [11]. Specifically, Foscan® prescribed for the palliative treatment of patients with advanced head and neck squamous cell carcinoma is applied in injectable form in an ethanol and propylene glycol mixture [12].Thus, there is a need to improve water solubility to facilitate porphyrin delivery and biodistribution using aqueous delivery systems without affecting their photochemistry.

An interesting and biocompatible option to enhance the aqueous solubility of compounds is conjugation with cyclodextrins (CDs). CDs are water soluble, enzymatically produced oligosaccharides consisting of α-D-glucopyranoside units that form a macrocycle with hydrophilic sides and a hydrophobic cavity. Their high biocompatibility has made them popular in pharmaceutics as well as in food and cosmetics [13]. CDs have been shown to improve the physicochemical properties of different drugs in the literature [14-18], and covalent conjugation of porphyrin-like molecules to CDs has been explored [19-22]. Thus, porphyrin-CD conjugates are highly interesting to facilitate drug delivery and improve photodynamic therapy.

The aim of this study was to explore the photophysical properties and investigate the biodistribution of a CD-*m*THPP

[a] Biomedical photonics group, Dept. of Chemistry and Molecular Biology, University of Gothenburg, Kemivägen 10, SE-412 96, Gothenburg, Sweden.
[b] Institute of Advanced Materials, Physicochemical Processes, Nanotechnology and Microsystems, National Centre for Scientific Research "Demokritos", Agia Paraskevi Attikis, 15310 Greece.
[c] Istituto per la Sintesi Organica e la Fotoreattività (ISOF), National Research Council (CNR), via Gobetti 101, 40129 Bologna, Italy.
[c] Chemical and Biological Engineering, Chalmers University of Technology, Kemivägen 10, SE-412 96, Gothenburg, Sweden.
* Corresponding authors; vladimir.kirejev@chem.gu.se; marica.ericson@chem.gu.se

conjugate *ex vivo*. We chose to covalently link the two macrocycles; i.e., the photo-inert βCD macrocycle and the photoactive *m*THPP ring, via a non-cleavable ether bond as illustrated in Figure 1. The rationale behind the design of the CD-*m*THPP conjugate is to provide aqueous solubility through the hydrophilic CD's moiety, preserving the photophysical properties of the *m*THPP's moiety. In addition, this conjugate has already demonstrated potential as a multimodal photosensitizer since the βCD cavity allows for accommodation of a co-drug [23]. Absorption, fluorescence, and fluorescence lifetime of the conjugate were assessed and compared to unconjugated *m*THPP. The cellular uptake in human squamous carcinoma cells (A431) was assessed in vitro by confocal microscopy and fluorescence lifetime imaging microscopy (FLIM). The *ex vivo* biodistribution of CD-*m*THPP was investigated after topical delivery to excised human skin using two-photon fluorescence microscopy (TPM) demonstrated proof-of-principle.

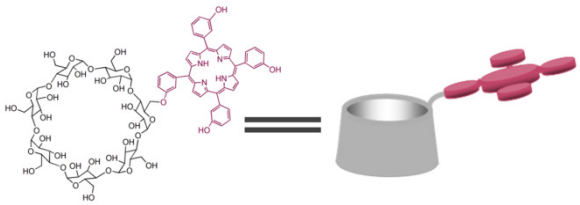

Figure 1. Chemical structure (left) of β-cyclodextrin-meso-tetra(m-hydroxyphenyl)porphyrin conjugate (CD-*m*THPP) and schematic drawing (right).

Results and discussion

The photophysical properties of CD-*m*THPP were investigated and compared with data for *m*THPP. Figure 2 presents the absorption and fluorescence spectra of CD-*m*THPP and *m*THPP in pure DMSO, 4% DMSO/PBS (v/v) and pure PBS. As observed from the spectra acquired in pure DMSO (Figure 2 A and C), the spectroscopic characteristics of *m*THPP are preserved for the CD-*m*THPP conjugate in agreement with an earlier study [23]. Noticeably, in the biocompatible solvents (Figure 2 B and D); i.e., PBS and 4% DMSO/PBS (v/v), the absorption spectra showing a lower FWHM and a higher intensity for the Soret band of the conjugate are indicative of a significantly lower degree of aggregation of CD-*m*THPP conjugate compared to *m*THPP. Moreover, no spectral data for *m*THPP in pure PBS could be obtained because of its lack of aqueous solubility. The fluorescence intensity of CD-*m*THPP in 4% DMSO/PBS (v/v) increased more than tenfold compared to *m*THPP, confirming improved solubility and lower degree of aggregation.

Absorption and steady-state fluorescence measurements were complemented by fluorescence lifetime measurements. Figure 3 shows the fluorescence decays for CD-*m*THPP and *m*THPP in the same solvents. Obvious from this figure is that the fluorescence decay of CD-*m*THPP is substantially prolonged in PBS and 4% DMSO/PBS (v/v) compared to *m*THPP. Decays have been fitted with multiexponential decay

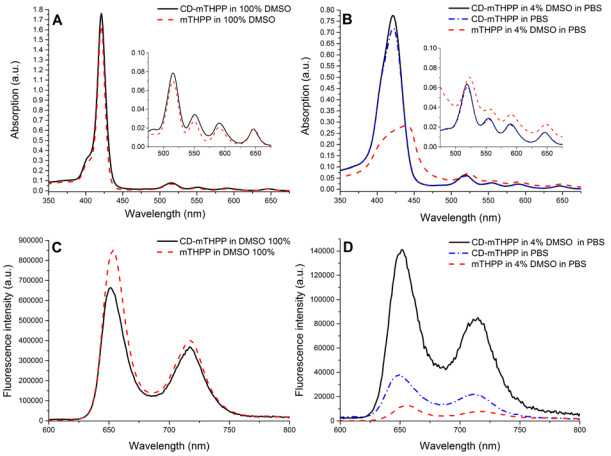

Figure 2. Absorption spectra of CD-*m*THPP and *m*THPP at 5 μM concentration in (A) pure DMSO and (B) PBS or 4% DMSO/PBS (v/v) and corresponding fluorescence spectra of CD-*m*THPP and *m*THPP at 407 nm excitation in (C) pure DMSO and (D) PBS or 4% DMSO/PBS (v/v). For the fluorescence measurements the absorbance at the Soret band maximum was fixed to 0.2 for all solutions.

functions, and the results are shown in Table 1. Multiexponential decay fitting was necessary as monoexponential fitting did not give satisfactory chi-square values indicative of the goodness of the fit. When *m*THPP was dissolved in pure DMSO, essentially only one species with long lifetime component (i.e., 10.5 ns) was found to contribute to fluorescence with a fractional intensity of 98%. This lifetime is in agreement for measurements on *m*THPP in methanol; i.e., 10.8 ns [8]. For *m*THPP in 4% DMSO/PBS a predominant (i.e., 90%) lifetime of 0.13 ns was observed. Assuming that *m*THPP is mainly present as monomers when dissolved in pure DMSO, we can assign the long lifetime component to the monomeric species and the short one to aggregates. When CD-*m*THPP conjugate was dissolved in the various solvents, fitting it with a triexponential function was necessary to obtain a good chi-square value. We can discern two lifetimes similar to those of *m*THPP and one intermediate (τ_3 = 1.4–2.4 ns). The fractional intensity of the long lifetime decreases going from DMSO to 4% DMSO/PBS (v/v) and PBS, and we observe an opposite trend for the shortest lifetime coherent with the aggregation behavior discussed above. Preexponential factors depend on several factors, among which the concentration of the different species in solution and confirms the different aggregation behaviours in aqueous solution of the model compound and the conjugate, the latter more readily dissolved as monomer or dimer in aqueous environment compared to unconjugated *m*THPP almost completely aggregated in 4% DMSO. The intermediate lifetime (τ_3) can be tentatively assigned to CD-*m*THPP conjugate in dimeric form [23]. Thus, the steady-state and time-resolved data nicely confirm the improved aqueous solubility of the CD-*m*THPP conjugate, compared to *m*THPP, and the improved photophysical properties in a biocompatible environment.

Table 1. Fluorescence lifetime data of CD-*m*THPP and *m*THPP in PBS, 4% DMSO/PBS (v/v) and pure DMSO at 5 μM concentration measured at 650 nm using excitation of 407 nm. τ_i – fluorescence lifetime; a_i – preexponential factors; f_i – fractional intensity at 650 nm of the single-lifetime components.

	τ_1, ns	$a_1(f_1)$	τ_2, ns	$a_2(f_2)$	τ_3, ns	$a_3(f_3)$	χ^2
CD-*m*THPP pure DMSO	0.10±0.01	0.27±0.01 (2.0%)	10.73±0.02	0.14±0.01 (95.4%)	2.40±0.22	0.02±0.01 (2.9%)	1.10
CD-*m*THPP 4% DMSO/PBS	0.14±0.01	0.41±0.01 (9.1%)	9.36±0.04	0.05±0.01 (74.1%)	1.42±0.05	0.07±0.01 (16.8%)	1.02
CD-*m*THPP PBS	0.12±0.01	0.48±0.01 (10.2%)	8.58±0.04	0.04±0.01 (69.1%)	1.55±0.05	0.07±0.01 (20.7%)	0.93
*m*THPP pure DMSO	0.15±0.02	0.17±0.01 (1.5%)	10.5±0.02	0.16±0.01 (98.5%)	-	-	1.07
*m*THPP 4% DMSO/PBS	0.13±0.01	0.70±0.01 (90.0%)	11.24±0.4	0.001±0.0001 (10.0%)	-	-	1.14

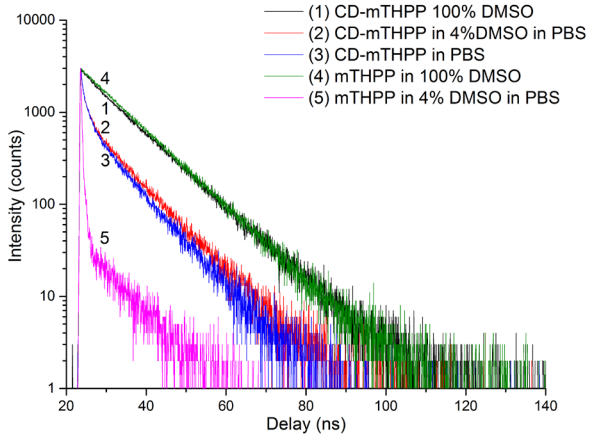

Figure 3. Fluorescence lifetime data of CD-*m*THPP complex and unconjugated *m*THPP dissolved in 4% v/v DMSO/PBS and pure DMSO (DMSO 100%). All concentrations are 5 μM. Fluorescence obtained using excitation at 407 nm and emission registered at 650 nm.

The cellular uptake of CD-*m*THPP was investigated in human squamous carcinoma (A431) using confocal fluorescence microscopy and FLIM. Figure 4A shows a confocal fluorescence image of a cluster of cells. The green channel demonstrates cellular autofluorescence, while the red channel corresponds to CD-mTHPP emission. Co-localization of green and red fluorescence implies that conjugate is present in the cytoplasm. No red fluorescence was detected from the cell nuclei. This implies predominantly cytoplasmic uptake. FLIM measurements (Figure 4B and C) revealed a dominating long-lifetime component; i.e., 10.3 ns, from the cytoplasm, which can be seen in green (Figure 4B) and red (Figure 4C). This lifetime is similar to the lifetime observed for monomeric CD-*m*THPP in solution, indicating that the CD-*m*THPP conjugate is present in the cells in monomeric form. Evident from Figure 4B and C is also the presence of clusters that exhibit a shorter average lifetime (~5 ns). These clusters were found both on the cell surface and within the cells (zoom in Figure 4 D and E). The clusters present within the cells can either have been taken up as clusters, or more likely, been formed during endocytosis. It should be noted that studies of cellular uptake of unconjugated *m*THPP using the same conditions was not possible due to the low emission intensity of the compound. Furthermore, it was observed that the cells were subject to photoactivation during the experiments, causing the cells to change their morphology, but without redistribution of compound.

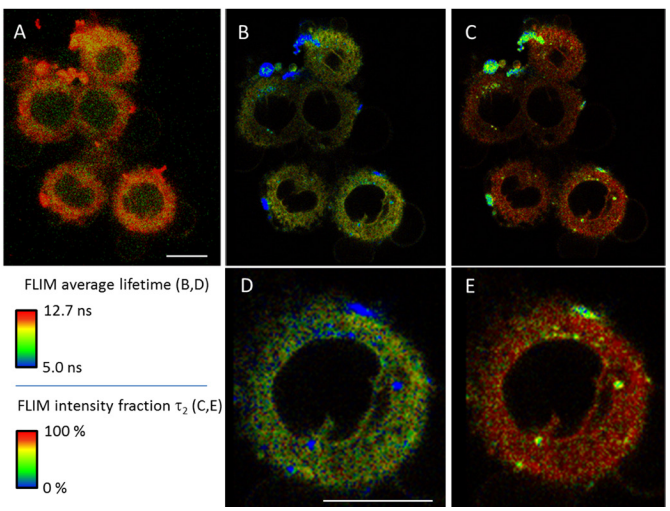

Figure 4. (A) Confocal fluorescence image of a cluster of A431 cancer cells incubated with 5 μM of CD-*m*THPP in 4% v/v DMSO/PBS showing overlay of cellular autofluorescence in green (500–550 nm) and CD-*m*THPP emission in red (660–740 nm). (B,C) FLIM images of the same cells with zoom in (D,E) acquired for 660–740 nm emission. (B,D) visualizing the average fluorescence lifetime, and (C,E) show the fractional intensity of the long-lifetime component τ_2. Excitation wavelength was 405 nm. Scale bars = 10 μm.

To assess the biodistribution *ex vivo*, the CD-*m*THPP conjugate and *m*THPP was topically administered to excised human skin and the fluorescence was visualized using TPM. The human skin is a challenging barrier for drug delivery, and topical delivery of compounds with molecular weight above 500 Da is generally considered difficult [24]. Thus it is expected that conjugation of *m*THPP (679 Da) to βCD (1135 Da), forming the conjugate (1796 Da), would decrease the possibility to deliver the compound to tissue; however, our experiments demonstrate the opposite. Figure 5 shows TPM images acquired from intact skin samples at different tissue

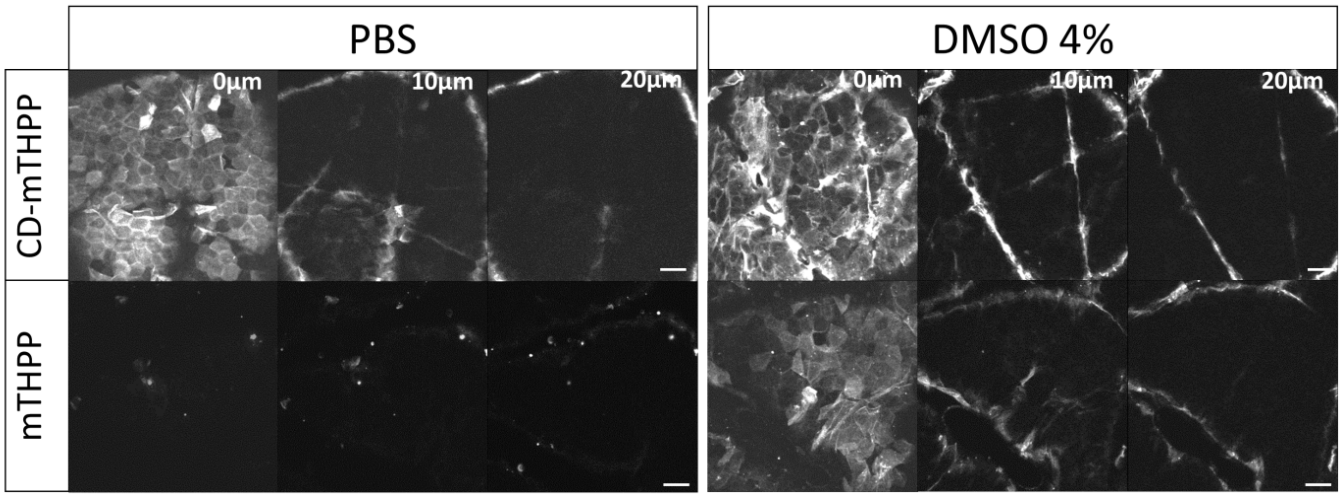

Figure 5 TPM images of human skin samples exposed to CD-mTHPP conjugate and mTHPP *ex vivo* for 20 h using PBS and 4% DMSO/PBS as vehicles. Images aquired en face to the skin surface at different dephts correspond to skin surface (0 µm), and upper epidermis (10 µm and 20 µm). Scale bar 50 µm. Excitation: 840 nm, emission: 590-710 nm.

depths. As can be seen in the figure, both CD-*m*THPP and *m*THPP penetrates the epidermis in the presence of DMSO (4%). In the context of the present work, we have used DMSO as a solvent and solubilizer. Presence of DMSO allowed comparing the skin penetration of CD-mTHPP and non-water soluble unconjugated mTHPP, but it should be noted that an effect of DMSO as skin penetration enhancer is expected [25]. Interestingly, the CD-*m*THPP conjugate shows a similar distribution pattern when administered using pure PBS, while no skin penetration was observed for *m*THPP in PBS, which was detected only as aggregates in the skin wrinkles. This implies that CD-*m*THPP, with its improved physicochemical properties, can be topically administered and diffuse into tissue.

TPM was also performed on tissue cross-sections of skin exposed to CD-*m*THPP and *m*THPP and subject to cryosectioning, as presented in Figure 6. The green fluorescence observed in the images originates from the endogenous autofluorescent features of the dermis; i.e., collagen and elastin [26], while the red signal from the upper epidermis corresponds to the fluorescence for CD-*m*THPP or *m*THPP. Similar to the experiments on intact skin samples, uptake of the compound in the upper epidermis was observed for both CD-*m*THPP and *m*THPP when it was administered in presence of DMSO (4%); while the uptake using pure PBS was only demonstrated for the CD-*m*THPP conjugate. In the case of *m*THPP in PBS, no uptake in the skin was observed. Fluorescence from *m*THPP was identified as aggregates on the very surface of the skin. Taken together, the results from the topical application in combination with TPM demonstrate how improved aqueous solubility of CD-*m*THPP facilitates biodistribution. Similar epidermal distribution was observed for free *m*THPP and the significantly larger CD-*m*THPP conjugate in the presence of DMSO. It is well known that lipophilicity and molecular weight are important factors to consider for skin permeability. The calculated octanol/water partitioning coefficient (log P) for the CD-*m*THPP conjugate at 3.7 ± 1.7, compared to 9.4 ± 1.5 for *m*THPP (using freeware ACD labs, Ontario, Canada), supporting the decreased lipophilicity and elevated aqueous solubility of the conjugate. In general, more lipophilic compounds are considered to exhibit improved skin partitioning [27]; however as lipophilicity and logP are linked with aqueous solubility, highly lipophilic compounds are demonstrating less skin permeability. Thus, the drawback of increasing the molecular weight by βCD conjugation seems to be outweighed by improved aqueous solubility.

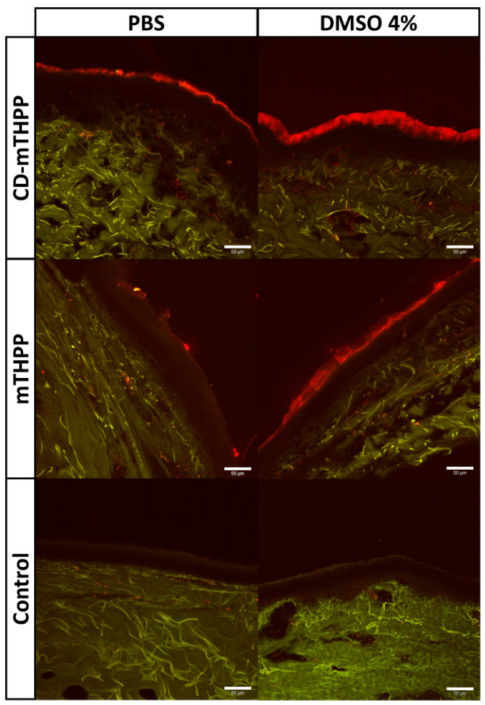

Figure 6 TPM images of cryosectioned human skin samples exposed to CD-*m*THPP conjugate and *m*THPP *ex vivo* for 20 h using PBS and 4% DMSO/PBS (v/v) as vehicles. Control samples were exposed only to PBS or 4% DMSO/PBS (v/v). Green channel (450-550 nm) mainly visualizes tissue autofluorescence, red channel (590-710 nm) mostly CD-*m*THPP or *m*THPP. Note that red structures in the dermis originate from autofluorescence and can be observed also in control samples (possibly flavins, lipo pigments or endogenous porphyrins [28]). Scale bars 50 µm. Excitation: 840 nm.

Conclusions

The aim of this study was to explore the improved aqueous solubility obtained by conjugating *m*THPP to β-CD with a special focus on biodistribution in human skin and squamous carcinoma cells. The photophysical properties of the CD-*m*THPP conjugate demonstrate significantly improved solubility of CD-*m*THPP in aqueous solution compared to unconjugated *m*THPP. FLIM verifies the cytosolic uptake of CD-*m*THPP, predominantly in the monomeric form, exhibiting a long fluorescence lifetime component. This finding is important to ensure efficient intersystem crossing producing a long-lived triplet state in a cellular environment, which is crucial for sparking a photodynamic effect. Furthermore, *ex vivo* administration of CD-*m*THPP to human skin demonstrates that delivery is not obstructed due to the larger molecular weight of the conjugate compared to free *m*THPP. On the contrary, the conjugate demonstrates improved biodistribution when delivered in an aqueous solution. To conclude, the results demonstrate the potential of CD-*m*THPP as a feasible strategy to gain improved biodistribution of a potent photosensitizer while conserving its intrinsic photochemical properties. In addition, the conjugate has the potential to act as a multifunctional system, where the βCD-unit allows for host-guest complexation that provids additional functionality, making the system highly interesting for future studies by means of improving photodynamic therapy.

Experimental

Synthetic procedures

All chemicals were purchased from Sigma Aldrich (Sigma Aldrich, Steinheim, Germany) unless stated differently. Spectroscopic-grade dimethylsulfoxide (DMSO) was used 1) as received or 2) diluted to 4% DMSO/PBS (v/v). *Meso*-tetra(*m*-hydroxyphenyl)-21,23*H*-porphyrin (*m*THPP) was purchased from Innochem (Innochem Ltd., Carnforth, Lancashire, UK). β-Cyclodextrin (βCD) was purchased from Sigma-Aldrich. 6-Monotosyl-β-cyclodextrin was prepared from β-cyclodextrin following a reported procedure [29].

CD-*m*THPP was prepared according to our established procedure, previously described in [23] with improvements, as follows: *meso*-tetra(*m*-hydroxyphenyl)-21,23*H*-porphyrin (61 mg, 0.089 mmol) was dissolved in dry (3 Å molecular sieves, 24 h) DMSO (2 mL) at 40° C under constant magnetic stirring, an argon atmosphere, and protected from light. Sodium hydroxide (23.5 mg, 0.59 mmol) was added and the reaction mixture was stirred for 15 min. 6-Monotosyl-β-cyclodextrin [29] (125.5 mg, 0.097 mmol) was dissolved in dry (3 Å molecular sieves, 24 h) DMSO (1.0 mL) and added to the reaction mixture in portions during 72 h, until all consumed [by TLC, (*i*-PrOH/EtOAc/H_2O/30% aq. NH_3, 5:3:3:1 (v/v), as the mobile phase]. The desired product appeared as a brown spot (R_f = 0.61), showed red fluorescence under ultraviolet light irradiation (λ_{ex} = 365 nm), and turned green upon spraying with a 4% sulfuric acid ethanolic solution. The reaction was stopped by the addition of HCl (1 M, 1.1 mL, to pH~6.0) and then ethanol/water (1:1, ~2 mL) and then the whole was dialyzed (benzoylated dialysis tubing, Sigma, MW_{CO}=2000) for ~ 1 day against distilled water. After removing the solvent, the dry material collected was washed extensively with ethyl acetate (100 mL) to remove unreacted *m*THPP and *m*THPP salts. The solid obtained was subjected to column chromatography using a long column (L x D = 60 cm x 2.4 cm) packed with silica gel (80 g) with *i*-PrOH/EtOAc/H2O/30% aq. NH_3 (5:3:3:1, v/v) as the elution system. Loading had to be restricted to a small portion of crude (~20 mg) per column. The first fraction collected was unreacted *m*THPP (20 mg in total) followed by CD-*m*THPP. Subsequently, the solvent was evaporated under vacuum, and the product was dialyzed once again after pH adjustment (1N HCl, 4<pH<5), affording CD-*m*THPP as a black powder (43 mg, 40% yield, based on reacted porphyrin). TLC (*i*-PrOH/EtOAc/H2O/NH3 (5:3:3:1): R_f = 0.61, and 1D/2D NMR spectra were identical to those reported before [23].

Skin sample preparation

Human skin specimens from Caucasian females, collected as leftovers from breast reduction surgery, were used in experiments. The specimens were prepared and examined using TPM according to earlier developed protocols [30, 31]. The skin samples were cut into 1 x 1 cm pieces, stored at -70 ° C and used within six months. The samples were thawed at room temperature before use. A major part of the subcutis was removed mechanically, using a scalpel. Afterwards, full-thickness skin samples were mounted in flow-through diffusion chambers for exposure to the different test solutions. The receptor compartment was filled with PBS, while the test solutions, which contained CD-mTHPP (5μM) or mTHPP (5μM) in PBS, 4% DMSO/PBS (v/v), or pure DMSO were added to the donor compartment. The diffusion chambers were sealed with parafilm and aluminum foil to exclude exposure to light. Partitioning of the compound into the skin sample was allowed for 20 hours at 30° C under constant stirring of the donor compartment. After exposure, samples were taken out of the diffusion chamber, thoroughly rinsed with PBS, and mounted on the microscopy slides using custom-made imaging chambers consisting of a cover slip and a double-sided sticky tape.

Skin sample cryosectioning

After skin sample incubation with the tested substances as described above, the same samples were transferred to freezing media O.C.T. (Tissue-tec, Torrance, CA, USA) and rapidly frozen in dry ice/ethanol. Frozen samples were cryo-sectioned (Leica 3050S, Nussloch, Germany) at -20 ˚C into 20 μm thick samples, transferred to microscopy slides and covered with a No. 1.5 cover slip (Menzel-Gläser, Braunschweig, Germany)

Cell culture preparation

$2x10^4$ human squamous carcinoma A431 cells (HPA cultures, Salisbury, UK) were seeded on a glass-bottomed petri

dish equipped with silicon inserts (diam. 1.2 cm, flexiPERM con A, Sarstedt, Sweden) 48 h prior to the experiment. Cells were kept in the full-growth media, which consisted of phenol red-free Eagles's Minimum Essential Medium (EMEM, Invitrogen, Pailsey, UK), supplemented with 10% fetal bovine serum, 2 mM glutamine EMEM, and 1% non-essential amino acids, at 37°C and in a 5% CO2 incubator. Before imaging, the full-growth media was substituted with the porphyrin solution; i.e., CD-*m*THPP (5μM) in 4% DMSO/PBS (v/v), and incubated for 2 h. Afterwards, the porphyrin solution was removed and the cells were gently rinsed with PBS. Cells were kept in PBS during imaging.

Absorption and fluorescence spectroscopy

UV-visible absorption spectra were recorded on a Varian Cary Eclipse 5000 spectrophotometer (Varian, Inc., USA). Fluorescence spectra were obtained on a Spex Fluorolog 111A (Horiba, Kyoto, Japan) spectrofluorometer. Right-angle detection was used. All experiments were carried out in quartz cuvettes of 1.0 cm path length.

Fluorescence lifetime measurement

Fluorescence decays were measured in air-equilibrated solutions for excitation at 407 nm (Hamamatsu pulsed laser; 59 ps pulse duration and 1 MHz repetition rate) using a time-correlated single photon counting system (TCSPC) (IBH Consultants Ltd., Glasgow, UK) with a resolution of 55 ps per channel. Photons were detected in right-angle configuration at a) 610 nm with a 550 nm cut-off filter and b) 650 nm with a 590 nm cut-off filter. Fluorescence decay profiles were analyzed with a least-squares method, using multiexponential decay functions and deconvolution of the instrumental response function. The software package was provided by IBH Consultants Ltd.

Confocal fluorescence microscopy and fluorescence lifetime imaging (FLIM)

Fluorescence lifetime imaging (FLIM) was performed on an inverted Nikon Ti-E microscope (Nikon Co., Shinjuku, Japan) laser scanning confocal microscope equipped with 488 nm and 640 nm CW lasers and a 405 nm pulsed/CW diode laser (PicoQuant GmbH, Berlin, Germany). Images were collected using a Nikon Plan Apo VC 60 oil immersion objective with NA 1.40. Filters were set to register the autofluorescence of cells at 500–550 nm and the fluorescence of the porphyrin at 660–740 nm.

Fluorescence lifetime imaging was performed with integrated PicoHarp 300 electronics (PicoQuant GmbH, Berlin, Germany) for TCSPC measurements. A single-photon avalanche diode detector equipped with a 625 to 675 nm band-pass filter was used for this scope. The repetition rate of the pulsed excitation at 405 nm was 40 MHz. The instrument response function of the system is approximately 220 ps. A tail fit was performed on the histogram, which was calculated for a region of interest of the sample image. Fluorescence decay profiles were analyzed with a least-squares method, using multiexponential decay functions. The fitting function used is

$$I(t) = b + \sum_j a_j e^{(-t/\tau j)} \qquad \text{with j ranging from 1 to 3}$$

The fractional intensity and the average fluorescence lifetime are calculated according to the following equations:

$$f_i = a_i\tau_i / \sum_j a_j\tau_j$$

$$\tau_{av} = \sum_j f_j\tau_j$$

Two-photon fluorescence microscopy (TPM)

Two-photon fluorescence images were obtained using s LSM 710 NLO microscope (Carl Zeiss, Jena, Germany) equipped with mode-locked femtosecond pulsed Mai Tai DeepSee laser and Plan-Apochromat 20x water immersion objective (NA 1.0) (Carl Zeiss, Jena, Germany). The excitation wavelength was set to 840 nm. Laser light intensity at the sample was in the range of 6–15 mW. Fluorescence was registered with descanned (internal) detectors with a fully opened pinhole. Band pass filters, 590–710 nm and 450–550 nm, were used to record signals of CD-*m*THPP and skin autofluorescence, respectively. 3D imaging was performed by acquiring z-stacks of images at different sample depths.

Acknowledgements

We acknowledge the Centre for Cellular Imaging, Sahlgrenska Academy, University of Gothenburg, for the use of their equipment and kind support of their staff, and the Centre for Skin Research (SkinResQU) for access to their cell culturing facility. We also thank Christina Halldin, Dermatology Department, Sahlgrenska University Hospital, for collecting the skin samples. Financial support was obtained from the Swedish Research Council and the Marie Curie ITN project N°237962 (CYCLON).

Notes and references

1. R. O. Potts and R. H. Guy, *Pharm. Res.*, 1995, **12**, 1628-1633.
2. W. J. Pugh, I. T. Degim and J. Hadgraft, *Int. J. Pharm.*, 2000, **197**, 203-211.
3. M. Förster, M. A. Bolzinger, H. Fessi and S. Briancon, *Eur. J. Dermatol.*, 2009, **19**, 309-323.
4. A. E. O'Connor, W. M. Gallagher and A. T. Byrne, *Photochem. Photobiol.*, 2009, **85**, 1053-1074.
5. J. S. McCaughan, Jr., J. T. Guy, W. Hicks, L. Laufman, T. A. Nims and J. Walker, *Arch. Surg.*, 1989, **124**, 211-216.
6. K. Kalka, H. Merk and H. Mukhtar, *J. Am. Acad. Dermatol.*, 2000, **42**, 389-413; quiz 414-386.
7. M. C. Berenbaum, R. Bonnett, E. B. Chevretton, S. L. Akande-Adebakin and M. Ruston, *Lasers Med. Sci.*, 1993, **8**, 235-243.
8. R. Bonnett, D. J. McGarvey, A. Harriman, E. J. Land, T. G. Truscott and U. J. Winfield, *Photochem. Photobiol.*, 1988, **48**, 271-276.
9. H. Ding, R. Mora, J. Gao and B. D. Sumer, *Otolaryngol Head Neck Surg*, 2011, **145**, 612-617.
10. M. C. Berenbaum, S. L. Akande, R. Bonnett, H. Kaur, S. Ioannou, R. D. White and U. J. Winfield, *Br. J. Cancer.*, 1986, **54**, 717-725.
11. B. Cunderlikova, E. G. Bjorklund, E. O. Pettersen and J. Moan, *Photochem. Photobiol.*, 2001, **74**, 246-252.
12. E. M. A. E. P. A. Reports.

13. E. M. M. Del Valle, *Process. Biochem.*, 2004, **39**, 1033-1046.
14. M. Cirri, M. Bragagni, N. Mennini and P. Mura, *Eur. J. Pharm. Biopharm.*, 2011.
15. P. Karande and S. Mitragotri, *Biochim. Biophys. Acta*, 2009, **1788**, 2362-2373.
16. K. A. Ansari, P. R. Vavia, F. Trotta and R. Cavalli, *AAPS PharmSciTech*, 2011, **12**, 279-286.
17. S. Samal and K. E. Geckeler, *Synth. Commun.*, 2002, **32**, 3367-3372.
18. K. Palaniappan, C. Xue, G. Arumugam, S. A. Hackney and J. Liu, *Chem. Mater.*, 2006, **18**, 1275-1280.
19. M. C. Gonzalez, A. R. McLntosh, J. R. Bolton and A. C. Weedon, *J. Chem. Soc. Chem. Commun.*, 1984, 1138-1140.
20. K. Kano, R. Nishiyabu, T. Yamazaki and I. Yamazaki, *J. Am. Chem. Soc.*, 2003, **125**, 10625-10634.
21. A. Puglisi, R. Purrello, E. Rizzarelli, S. Sortino and G. Vecchio, *New. J. Chem.*, 2007, **31**, 1499-1506.
22. T. Kiba, H. Suzuki, K. Hosokawa, H. Kobayashi, S. Baba, T. Kakuchi and S. Sato, *J. Phys. Chem. B*, 2009, **113**, 11560-11563.
23. A. Fraix, A. R. Gonçalves, V. Cardile, A. C. E. Graziano, T. A. Theodossiou, K. Yannakopoulou and S. Sortino, *Chem. Asian J.*, 2013, **8**, 2634-2641.
24. J. D. Bos and M. M. Meinardi, *Exp Dermatol*, 2000, **9**, 165-169.
25. A. C. Williams and B. W. Barry, *Adv. Drug Delivery. Rev.*, 2004, **56**, 603-618.
26. M. B. Ericson, C. Simonsson, S. Guldbrand, C. Ljungblad, J. Paoli and M. Smedh, *Journal of Biophotonics*, 2008, **1**, 320-330.
27. M. Chen, X. Liu and A. Fahr, *International Journal of Pharmaceutics*, 2011, **408**, 223-234.
28. G. A. Wagnieres, W. M. Star and B. C. Wilson, *Photochem. Photobiol.*, 1998, **68**, 603-632.
29. B. Brady, N. Lynam, T. O'Sullivan, C. Ahern and R. Darcy, *Org. Synth.*, 2000, **77**, 220-224.
30. J. Bender, C. Simonsson, M. Smedh, S. Engström and M. B. Ericson, *J. Control. Release.*, 2008, **129**, 163-169.
31. C. Simonsson, S. I. Andersson, A. L. Stenfeldt, J. Bergström, B. Bauer, C. A. Jonsson, M. B. Ericson and K. S. Broo, *J. Invest. Dermatol.*, 2011, **131**, 1486-1493.